

Design of a New Step-like Frame FBAR for Suppression of Spurious Resonances

Puneet KUMAR, Chandra Charu TRIPATHI

Dept. of Electronics and Communication Engineering, UIET, Kurukshetra University, Kurukshetra, India

puneet.kumar04@gmail.com, tripathiuiet@gmail.com

Abstract. Film bulk acoustic wave resonators (FBARs) are of great interest for wireless applications due to its inherent advantages at microwave frequencies. However, the presence of spurious modes near the main resonance degrades the performance of resonators and requires development of new methods to suppress such unwanted modes. Different techniques are used to suppress these spurious modes. In this paper, we present design of a new step-like frame structure film bulk acoustic wave resonator operating near 1.5 GHz. The simulated results are compared with simple frame-like structure. The spurious resonances are eliminated effectively and smooth pass band is obtained with effective coupling coefficient of 5.68 % and quality factor of 1800. The equivalent electrical mBVD model of the FBAR based on impedance response is also presented. These highly smooth phase response and passband skirt steepness resonators are most demanding for the design of low cost, small size and high performance filters, duplexers and oscillators for wireless systems.

Keywords

Film bulk acoustic wave resonator, step-like frame, spurious resonance, effective coupling coefficient, COMSOL Multiphysics.

1. Introduction

In the recent years, there has been rapid growth in the wireless communication systems at RF/microwave frequency region. These systems require small size, high performance and increased level of circuit complexity for system on chip and ease of portability. Most of the microwave devices such as filter, duplexer and oscillator require film bulk acoustic resonator (abbreviated as FBAR) as a key component for their design due to its small size, low cost, high Q and high power handling capability [2].

The most basic configuration of film bulk acoustic resonator (FBAR) is very similar to the basic quartz crystal scaled down in size [2]. It consists of a thin film of piezoelectric material sandwiched between two metal electrodes

as shown in Fig. 1 (a). When an alternating electric potential is applied to a piezoelectric material, it produces mechanical deformation. The FBAR acts as an acoustic cavity resonator in which the acoustic wave bouncing back and forth between walls $\lambda/2$ apart upon proper excitation. The walls or electrodes (e.g. Al, Au etc.) act as acoustic impedance discontinuities and the medium filling the cavity is a piezoelectric material (e.g. ZnO, AlN etc.). The electrical impedance response of FBAR has two resonant frequencies i.e. series resonant frequency where impedance is minimum and parallel resonant frequency where impedance is maximum. The ideal impedance response of FBAR is shown in Fig. 1 (b).

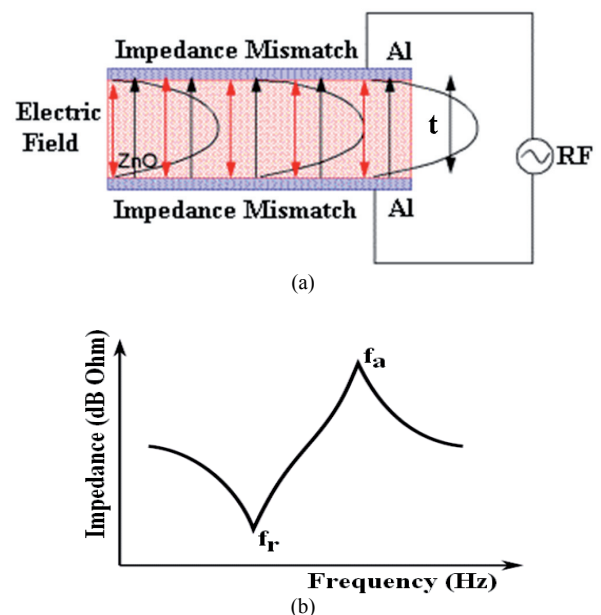


Fig. 1. (a) Excitation of acoustic resonator by an electric field in thickness direction; (b) Ideal electrical input impedance response of FBAR.

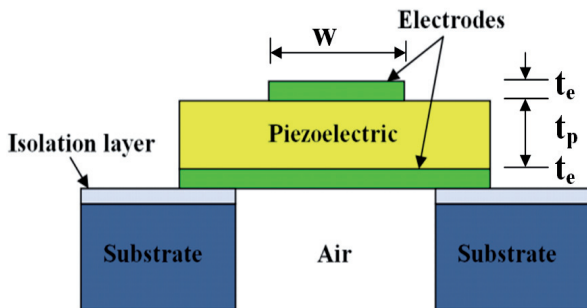
The acoustic waves that propagate in FBAR are thickness excited waves which propagate parallel to the electric field and the lateral excited waves which propagate perpendicular to the electric field. Because FBARs utilize thickness excited waves for their operation, the lateral waves are undesirable and generate spurious modes which may degrade the performance of resonator which in turn affects the performance of filters, oscillators etc.

To suppress the generation of spurious modes different techniques are presented so far [3-10]. In the apodization technique, the top electrode is designed with non-parallel edges which increases the resonant path and leads to more attenuated modes and thus degrades the strength of spurious lateral modes [4-10]. Another technique in which a viscoelastic acoustic damping material is placed along perimeter of the electrodes to attenuate reflections of the lateral acoustic modes at the electrode edges [5]. Another method is the application of frame-like region in which the edges of the top electrode are thickened which prevent the spurious lateral mode excitation, thus provide the spurious free resonator and confine the energy within the active area [1], [6]. In order to suppress spurious resonance, in one of the approach, a thinner bottom electrode of Al is designed and the bottom electrode to form frame-like air gap structure is applied [8], [9].

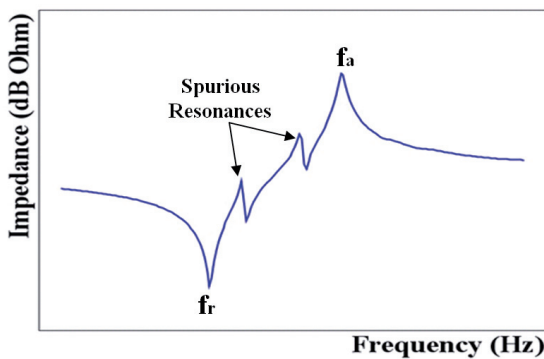
Instead of simple frame structure, the step-like frame may result in optimum mass loading so that spurious resonances can be effectively suppressed. Keeping this in view in this paper, we propose a new step-like frame structure for spurious resonance suppression. The result of above both frame FBARs is presented and compared with optimized result available in literature. The equivalent mBVD model of FBAR is also presented.

2. Film Bulk Acoustic Resonator

Fig. 2 (a) represents a typical FBAR structure.



(a)



(b)

Fig. 2. (a) Schematic of a typical FBAR structure; (b) Impedance characteristic with spurious lateral resonances.

The performance of a film bulk acoustic wave resonator is analyzed by the impedance characteristics of the resonator. The impedance of a resonator is characterized by two resonances: first at the resonance frequency (f_r) where the magnitude of the impedance tends to its minimum value and the second at anti-resonance frequency (f_a) where the magnitude of the impedance is maximum. The fundamental resonance frequency ($f_{r,t}$) of thickness excited FBAR is roughly given by:

$$f_{r,t} = v / \lambda = v_T / 2t \tag{1}$$

where v_T is the velocity of fundamental thickness mode, λ is the acoustic wavelength and $\lambda = 2t$, t is the thickness of the device.

The relationship between acoustic impedances, acoustic velocity and thickness of electrode and piezoelectric material is given by:

$$Z_e / Z_p = \tan \theta_e \cdot \tan \theta_p \tag{2}$$

where $\theta_e = k_e \cdot t_e$; $\theta_p = k_p \cdot (t_p/2)$; $k_e = \omega_a/v_a$; and $k_p = \omega_a/v_D$; in which Z_e and Z_p are the acoustic impedance of electrode and piezoelectric material; t_e and t_p are the electrode and AlN thickness respectively; v_a and v_D are the acoustic velocity of electrode and AlN respectively; $\omega_a = 2\pi f_a$, f_a is the anti-resonant frequency. The FBAR has air interface at top and bottom electrode for acoustic isolation and resembles to the stepped impedance resonator as in [11].

The resonance frequency of lateral modes ($f_{r,l}$) is approximated by:

$$f_{r,l} = N (v_L / 2w) \tag{3}$$

where N is the mode number, v_L is the velocity of lateral modes, w is the distance between electrode edges [10].

In FBAR, because the lateral dimension w is much larger than the thickness t of the resonator, the higher harmonics of the lateral excited modes may appear close to the resonance frequency of the thickness mode and show up as ripple between the resonance and anti-resonance frequency of the resonator and deteriorate the resonator performance as shown in Fig. 2 (b).

The effective coupling coefficient is an important parameter for performance analysis of FBAR. It is directly related to the difference between resonant frequency (f_r) and anti-resonant frequency (f_a). The effective coupling coefficient of FBAR is given by:

$$k_{eff}^2 = (\pi^2 / 4) \times [(f_a - f_r) / f_a]^2 \tag{4}$$

The coupling coefficient depends on the piezoelectric material parameters, thickness of the metal electrodes and fabrication process also [12].

The quality factor is a measure of loss in a resonator. It determines the sharpness of the resonance peak and the steepness of the pass band skirt. Higher Q value is desired for the higher selectivity of a resonator. The quality factor of FBAR is determined by:

$$Q = f_r / \Delta f_{(3dB)} \tag{5}$$

where f_r is the resonant frequency and $\Delta f_{(3dB)}$ is the relative bandwidth of the resonator. mBVD model of FBAR is also presented.

3. FBAR Modeling and Simulation Results

In this paper, we use the COMSOL Multiphysics software to simulate the response of FBAR. The 2-D geometric model of FBAR along with mechanical and electrical boundary conditions is shown in Fig. 3.

The piezoelectric material used is aluminum nitride (AlN) with thickness (t_p) of 3 μm and aluminum is used for both top and bottom electrode. The thickness of top and bottom electrode (t_e) is same and is equal to 0.3 μm . The area of top electrode is $220 \times 220 \mu\text{m}^2$. The resonator is formed by the overlapped area of top and bottom electrode with AlN sandwiched between them.

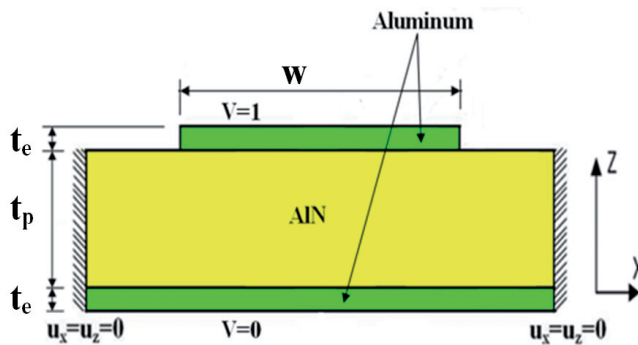


Fig. 3. 2-D geometric model of FBAR with mechanical and electrical boundary conditions.

The material properties used for the simulation contain anisotropic properties for AlN are $c_{11} = 345$, $c_{12} = 125$, $c_{13} = 120$, $c_{22} = 345$, $c_{23} = 120$, $c_{33} = 395$, $c_{44} = 118$, $c_{55} = 118$, $c_{66} = 110$ [GPa]; $e_{15} = -0.48$, $e_{31} = -0.58$, $e_{33} = 1.55$ [C/m²]; $\epsilon_{11} = 9$, $\epsilon_{22} = 9$, $\epsilon_{33} = 11$, where [c] corresponds to stiffness matrix, [e] corresponds to piezoelectric matrix and [ϵ] corresponds to permittivity matrix. The density of AlN has been set to 3512 kg/m³. For the aluminum electrodes, the Young's modulus has been set to $E = 69$ GPa, Poisson ratio has been set to 0.35 and density $\rho = 2700$ kg/m³. For SiO₂ layer, Young's modulus has been set to $E = 70$ GPa, Poisson ratio = 0.17 and density $\rho = 2200$ kg/m³ [1], [12]. The mechanical boundary condition ($u_x = u_z = 0$) at the edges represents that the horizontal and vertical displacement are assumed to be zero and absorbing boundaries are used at the edges to avoid the reflection due to truncated domain for FEM analysis. The electrical boundary conditions $V = 1$ and $V = 0$ are used to set the potential difference of 1 V between the top and bottom electrodes.

The acoustic losses of the piezoelectric material are accounted by using damping factor equal to 5.6e-4, and

dielectric loss = 0.2%. For the simulation of FBAR, the substrate is not included and the corresponding boundary conditions are provided as the thickness of substrate is very high than the resonator thickness and it requires large simulation time and high system capabilities. The frequency response analysis of FBAR is performed in MEMS module of COMSOL Multiphysics for piezoelectric material response analysis.

3.1 FBAR without Frame Structure

First, we simulate the FBAR without frame with dimensions as shown in Fig. 3. In conventional FBAR structures, the whole energy is not trapped in the electrode region leading to some of the trapped energy leaks into non-electroded region which causes spurious resonances [3]. The electrical input impedance response of no frame FBAR shows some spurious resonances between series and parallel resonance frequencies as shown in Fig. 4 (a). The impedance phase response in Fig. 4 (b) shows phase ripples between series and parallel resonance frequencies.

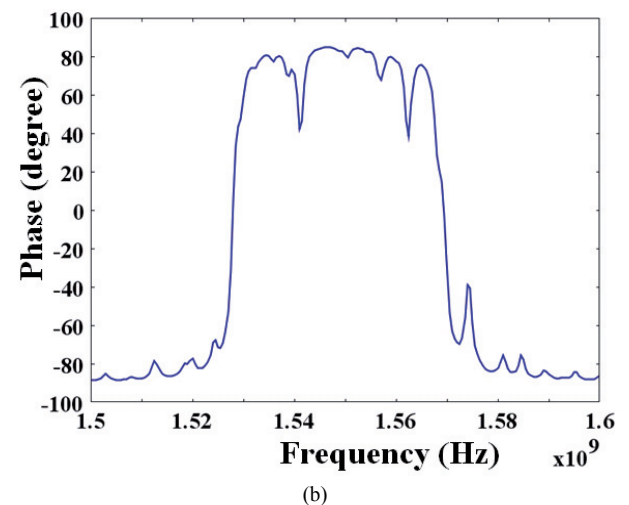
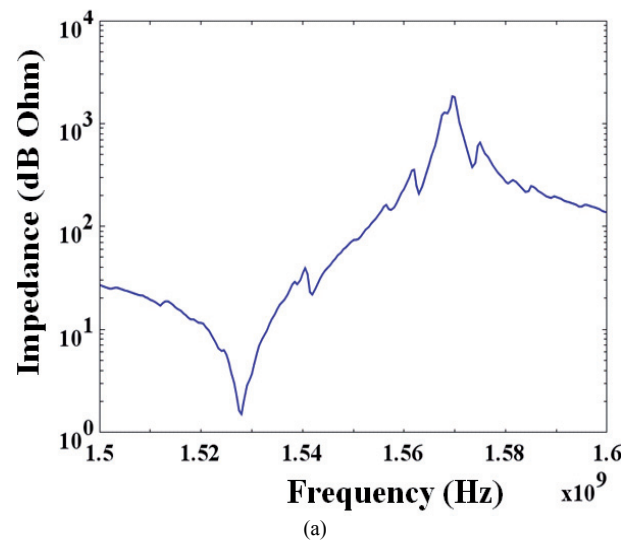


Fig. 4. (a) Impedance response of no frame FBAR; (b) Phase response of no frame FBAR.

3.2 Simple Frame FBAR

Earlier discussion to suppress the spurious resonance includes simple frame-like FBAR structures in which the top electrode is thickened at its edges with uniform width and thickness which confines the center area of the resonator as shown in Fig. 5. The width and thickness of the frame-like electrode are varied to obtain flat displacement profile for piezoelectrically excited strongest resonance mode in the center area of the resonator and suppress the lateral waves due to increased mass loading. The mass loading at the edges due to frame-like structure also helps in trapping the maximum energy in the active area and avoids the generation of unwanted lateral modes [3], [6]. It is observed that the simple frame could not eliminate small ripples effectively as small ripples are present in the phase response. For the comparison purpose phase response of a particular simple frame FBAR is shown in Fig. 6 with optimum frame width (w_f) and thickness (t_f) of $9\ \mu\text{m}$ and $0.3\ \mu\text{m}$ respectively as reported in literature [1]. In this paper, instead of simple frame-like structure FBAR, step-like-frame FBAR is designed and then optimized as shown in Fig. 7.

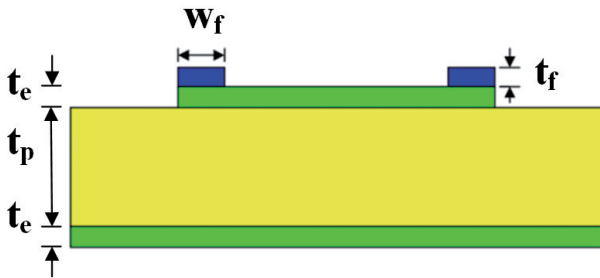


Fig. 5. Simple frame FBAR structure.

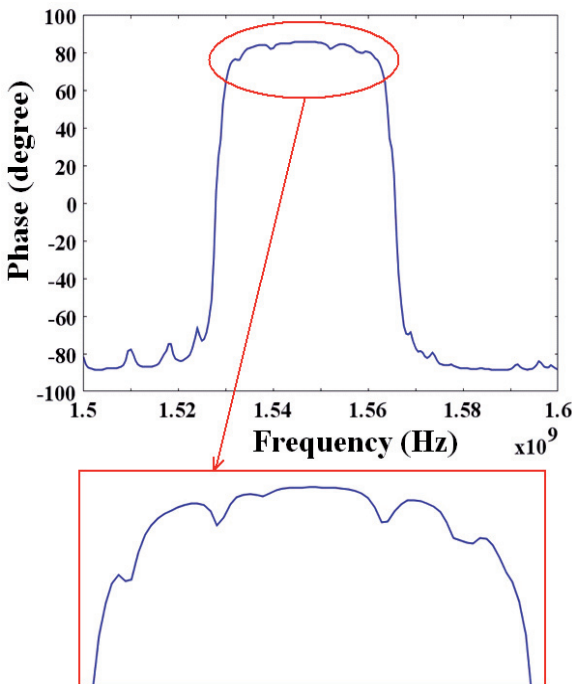


Fig. 6. Phase response of simple frame FBAR.

3.3 Step-like Frame FBAR

Step-like frame FBAR is shown in Fig. 7. It is a modified form of simple frame FBAR in which the frame

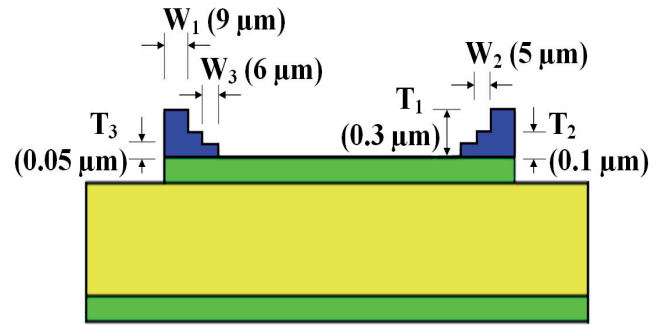


Fig. 7. Step-like frame FBAR structure.

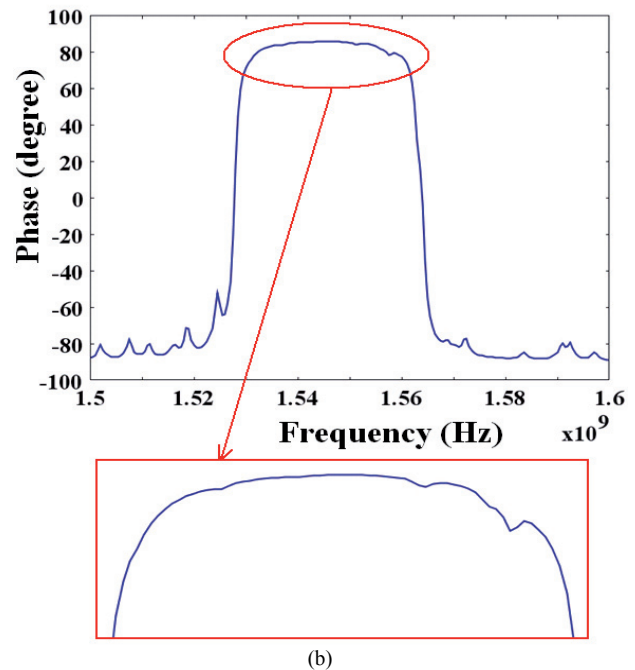
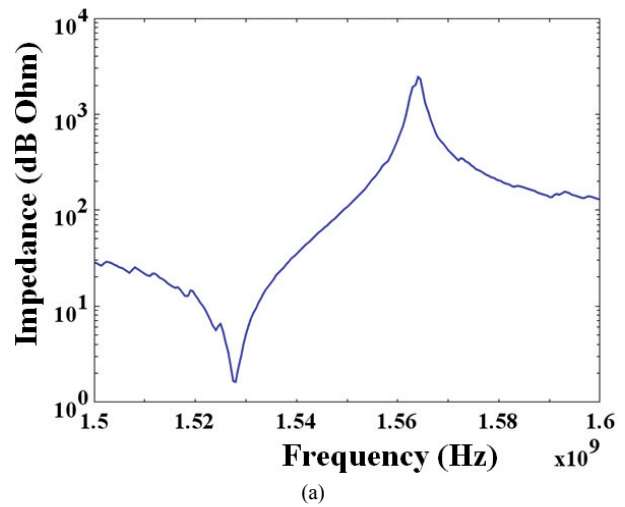


Fig. 8. Step-like frame FBAR: (a) Impedance magnitude response; (b) Phase response.

is designed in the form of step shape. It is considered that due to step shape the total mass loading on the top electrode is varied in steps as compared to simple frame electrode so that small ripples can be eliminated also and better performance can be obtained than simple frame FBAR. The smaller steps help in precisely smoothing the phase response. The phase ripples in the passband can increase or decrease as the dimension of each step varies. When the dimension of a step is narrower than the optimum value, it leads to a series of spurious resonances above resonant frequency. When the dimension of a step increases beyond the optimum value, the spurious resonances increase above and below the resonant frequency and effective electromechanical coupling coefficient decreases rapidly. Also, as the number of steps increases the anti-resonant frequency shift downward as the effective electromechanical coupling coefficient decreases due to increased mass loading. On the other hand, the increased mass loading suppress the generation of unwanted lateral modes and helps in energy trapping. So, the number of steps and the width and thickness of each step are varied to obtain the optimum performance.

For the simulation of the step-like frame FBAR, an Al step-like frame is placed on the edges of the top electrode. The width of each step is varied from $1\text{e-}6$ m to $12\text{e-}6$ m and thickness varied from $0.05\text{e-}6$ m to $0.4\text{e-}6$ m to obtain the improved result. The optimum result is obtained for thickness $T_1 = 0.3\text{e-}6$ m, $T_2 = 0.1\text{e-}6$ m, and $T_3 = 0.05\text{e-}6$ m and width $W_1 = 9\text{e-}6$ m, $W_2 = 5\text{e-}6$ m, and $W_3 = 6\text{e-}6$ m. The input impedance and phase response of step-like frame FBAR are shown in Fig. 8 (a) and 8 (b) respectively which show that the spurious resonances are suppressed and smooth passband is obtained which is desirable for low noise filter applications.

4. Performance Comparison

The performances of all the FBAR structures are compared to analyze the spurious resonance present impedance response. In no frame FBARs, the ripples are very large as shown in Fig. 4 (b). In simple frame FBARs, the stronger phase ripples are effectively removed but small ripples are still present as clearly shown in inset in Fig. 6. In step-like frame FBAR, a smoother phase response is obtained because the small ripples are also removed as clearly seen in inset in Fig. 8 (b). The comparison of impedance responses and phase responses of all FBARs are shown in Fig. 9 (a) and (b) respectively.

As shown in Fig. 9, the resonant frequencies of all the FBAR structures are same whereas the anti-resonant frequency decreases downward due to increased mass loading. This increased mass loading reduces the spurious modes. The quality factor of all FBARs is nearly equal to 1800 at resonant frequency which is sufficient for designing highly selective bandpass filters and duplexers. When the area of the edge load is large, anti-resonance frequency

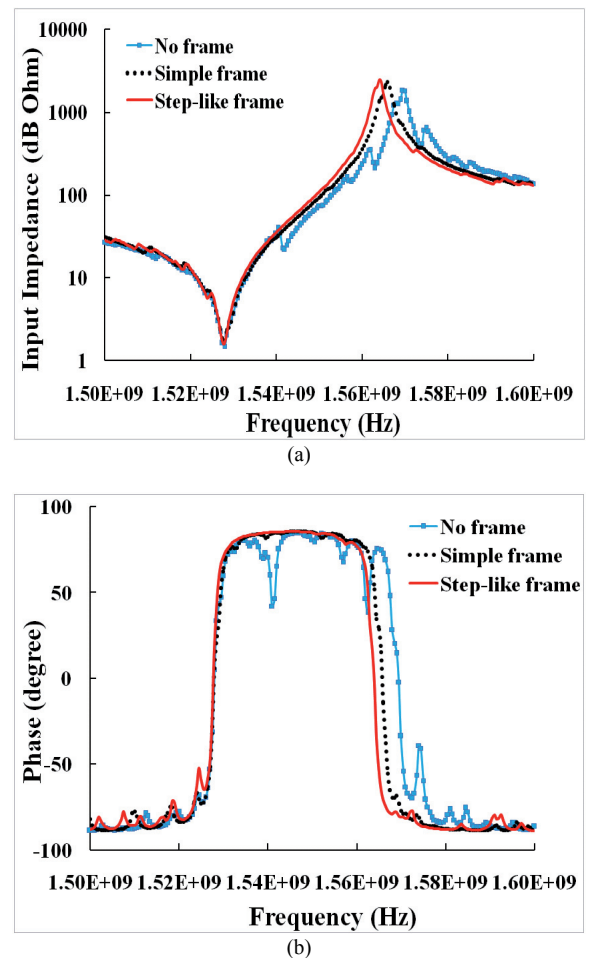


Fig. 9. (a) Comparison of impedance responses; (b) Comparison of phase responses.

allocation deviates to lower values because of a resonant mode present in the electrical behavior of the FBAR resonator and leak of the energy contained in the fundamental mode to the surrounding region as reported in literature [3]. This in terns also reduces effective electromechanical coupling constant [3]. Recently, a work on FBAR using AlN piezoelectric layers have been reported at X-band frequency around 8 GHz [12]. The advantage of using AlN layers is that it can be easily deposited on high-resistivity silicon wafers by magnetron sputtering, which offers compatibility with conventional semiconductor technology. This enables possibility of integration of different passive and active circuits by the processes of MEMS, nanolithography, micromachining techniques resulting high-quality self-sustainable membranes, increased resonance frequency of FBAR structures [12].

5. Equivalent Electrical Model

The equivalent mBVD model basically consists of two parallel branches i.e. motional arm and static capacitance arm. The motional arm comprises the series motional inductance L_m , capacitance C_m , and resistance R_m . L_m represents the acoustic mass; while C_m and R_m represent

the compliance and acoustic loss respectively. The static capacitance branch is formed by the parallel-plate capacitance C_0 formed between the top and bottom electrodes separated by a dielectric (i.e. piezoelectric crystal) of FBAR and R_p is serially added to C_0 to account for the dielectric loss in the piezoelectric film. R_s represent the resistance in connecting transmission lines [13]. The relation between series resonant frequency (f_s) and parallel resonant frequency (f_p) and lumped electrical parameters is given by:

$$f_s = \frac{1}{2\pi\sqrt{L_m C_m}}, \tag{6}$$

$$f_p = \frac{1}{2\pi\sqrt{L_m\left(\frac{C_0 C_m}{C_0 + C_m}\right)}}. \tag{7}$$

To validate the simulation results of above designed FBARs the equivalent electrical mBVD models are also designed and their response compared with simulation results which shows good agreement between both results. The equivalent electrical model for thickened edge load solution (simple frame) proposed in [3] is also tried for simple frame FBAR with AlN as piezoelectric material. This model does not fit to the simulated results as there is no resonance created other than the main resonance far above or below in the impedance response. So, the approach applied in [3] that the new resonance mode is created in the electrical behavior is not valid in our case. However, the response of FBAR with large frame width shows a new resonating mode below the main resonance in the electrical impedance response. In our simulation results with varying frame width, we observe that a new resonating mode will be present due to frame when the resonator width to thickness ratio is nearly 8:1 or less. We also observed that if the resonator area is smaller than the resonator area in our case; more energy leakage to the surrounding region can happen for large resonator width to frame width ratio.

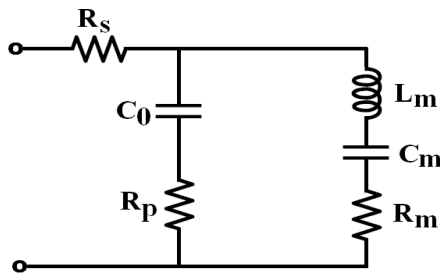


Fig. 10. Equivalent electrical model.

The equivalent electrical mBVD model for the step-like frame FBAR and comparison between simulated and equivalent circuit impedance response in a wider frequency range is shown in Fig. 10 and Fig. 11. The calculated values of $L_m = 1.45e-7$ H, $C_m = 7.49e-14$ F, $R_m = 0.773$ Ω , $C_0 = 1.57e-12$ F, $R_p = 0.002$ Ω . R_s is considered zero as no connecting transmission line is included in the modeling. Both results show good agreement in terms of resonant

frequencies. As mBVD is a 1-D model and it does not consider lateral resonances effects.

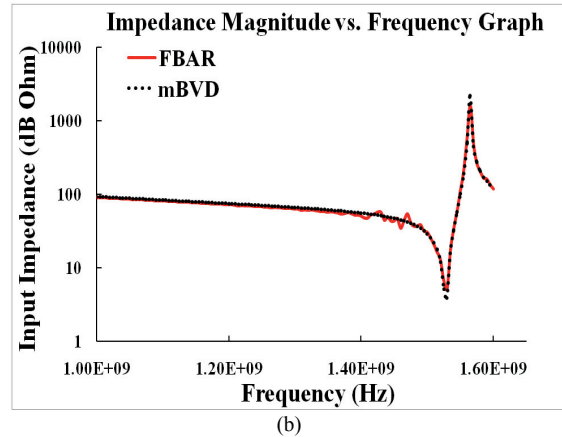


Fig. 11. Comparison between simulated and equivalent circuit impedance response.

6. Conclusion

Simulation of FBARs without frame, with simple frame, and a new step-like frame structure has been done using COMSOL Multiphysics software which is based on finite element modeling. Simple frame electrodes with optimum width and thickness remove large ripples between series and parallel resonant frequencies but small ripples still remain present. Using the step-like-frame with appropriate dimensions, the spurious resonances are eliminated effectively. However, inappropriate dimensions may lead to large spurious modes. The designed step-like FBAR has effective coupling coefficient of 5.68 % and quality factor of 1800. As the resonator width to frame width ratio is larger for optimum dimensions in step-like frame so energy leakage does not show any other resonant mode due to frame region. The obtained mBVD model shows very good agreement with simulated result. These FBARs are highly useful for the design of low cost, small size and high performance filters, duplexers and oscillators for wireless systems.

Acknowledgements

Authors are thankful to Prof. Dinesh Kumar, Director, UIET, KUK for his immense support throughout the work. The authors are also thankful to “NPMASS” for funding and setting up a design center for research in MEMS/NEMS at Electronic Science Dep., Kurukshetra University.

References

[1] LEE, J. H., YAO, C. M., TZENG, K. Y., CHENG, C. W., SHIH, Y. C. Optimization of frame-like film bulk acoustic resonators for

- suppression of spurious lateral modes using finite element method. In *IEEE Ultrasonics Symposium*, 2004, vol. 1, p. 278 – 281.
- [2] MAHON, S., AIGNER, R. Bulk acoustic wave devices – why, how, and where they are going. In *CS MANTECH Conference*. Austin, Texas (USA), May 14 - 17, 2007, p. 15 – 18.
- [3] VERDU, J., PACO, P., MENENDEZ, O. Electric equivalent circuit for the thickened edge load solution in a bulk acoustic wave resonator. *Progress in Electromagnetics Research M*, 2010, vol. 11, p. 13 – 23.
- [4] LARSON, J., RUBY, R., BRADLEY, P. Method for reducing lateral modes in FBARs. *U.S. Patent* 6215375.
- [5] CRAWDFORD, J. D., CUSHMAN, D. Semiconductor bulk acoustic resonator with suppressed lateral modes. *U.S. Patent* 6381820.
- [6] KAITILA, J., YLILAMMI, M., ELLA, J., AIGNER, R. Spurious resonance free bulk acoustic wave resonators. In *Proceeding of IEEE Ultrasonics Symposium*, 2003, p. 84 – 87.
- [7] AIGNER, R. MEMS in RF filter applications: Thin-film bulk acoustic wave technology. *Sensor Update*, 2003, vol. 12, p. 175 to 210.
- [8] OHARA, R., YANASE, N., YASUMOTO, T., KAWASE, M., MASUKO, S., OHNO, T., SANO, K. Suppression of acoustic energy leakage in FBARs with Al bottom electrode: FEM simulation and experimental results. In *IEEE Ultrasonics Symposium*, 2007, p. 1657 - 1660.
- [9] YANG, W., TAM, W. Spurious wave suppression in BAW resonators with frame-like airgap. In *IEEE International Frequency Control Symposium*, June 1 - 4, 2010, p. 656 – 660.
- [10] ROSEN, D., BJURSTROM, J., KATARDJIEV, I. Suppression of spurious lateral modes in thickness-excited FBAR resonators. *IEEE Transactions on Ultrasonics, Ferroelectrics and Frequency Control*, July, 2005, vol. 52, no. 7, p. 1189 – 1192.
- [11] LEE, S. Y. Optimum resonant conditions of stepped impedance resonators. In *European Microwave Conference*, 2005.
- [12] LANZ, R., MURALI, P. Bandpass filters for 8 GHz using solidly mounted bulk acoustic wave resonators. *IEEE Transactions on Ultrasonics, Ferroelectrics and Frequency Control*, June 2005, vol. 52, no. 6, p. 936 – 946.
- [13] CAMPANELLA, H. *Acoustic Wave and Electromechanical Resonators: Concept to Key Applications*. Norwood: Artech House, 2010.

About Authors ...

Puneet KUMAR received the B. Tech (Hons.) and M. Tech degree in Electronics and Communication Engineering from Kurukshetra University, Kurukshetra, India, in 2010 and 2012. His research interests include thin film bulk acoustic wave resonators and filters.

Chandra Charu TRIPATHI received the M.Sc. (Solid State Electronics Devices) degrees from Bannaras Hindu University, Varanasi, India, in 1987 and Master in Engineering (Microelectronics) in the year 1991 from BITS, Pilani, India. From 1991 to 2003, he was associated with Haryana State Electronics Development Corporation (HARTRON). In the year 2003, he joined ACE&AR Ambala (a Kurukshetra University, Kurukshetra, affiliated engineering college) as Assistant Professor (Reader) and served up to July 2007. In the year 2007, he moved to the University Institute of Engineering & Technology (UIET) Kurukshetra University, Kurukshetra and since then heading the Department of Electronics and Communication Engineering. He received his Ph.D. in Electronics from Kurukshetra University, Kurukshetra, India in the year 2009. His research interests include optoelectronics products, optical networks, optical devices, optical fiber communications, sensor networks, MANETS, microwave propagation, antenna, VLSI devices/ technology Bio-MEMS/RF MEMS devices. He is a semiconductor technologist and a reviewer for many journals.